The Nazca–South America Euler vector and its rate of change

Eric Kendrick[a], Michael Bevis[a,*], Robert Smalley Jr.[b], Benjamin Brooks[a],
Rodrigo Barriga Vargas[c], Eduardo Lauría[d], Luiz Paulo Souto Fortes[e]

[a]*School of Ocean and Earth Science and Technology, University of Hawaii, 1680 East West Road, Honolulu, HI 96822, USA*
[b]*Center for Earthquake Research, University of Memphis, Memphis, TN, USA*
[c]*Instituto Geográfico Militar de Chile, Santiago, Chile*
[d]*Instituto Geográfico Militar de Argentina, Buenos Aires, Argentina*
[e]*Instituto Brasileiro de Geografia e Estatística, Rio de Janeiro, Brazil*

Abstract

We present velocities relative to the South American plate for five GPS stations on the Nazca plate and use these measurements to estimate the modern Euler vector. We find a pole at 55.8°N, 92.5°W with a rotation rate of 0.60 °/Myr. Because the GPS station at Easter Island appears to be moving at approximately 6.6 mm/yr relative to the other Nazca stations, we repeat our analysis with this station excluded from the inversion to obtain a second and preferred result (called CAP10) with a pole at 61.0°N, 94.4°W and a rate of 0.57 °/Myr. We compare these results with published finite rotation vectors and infer that during the past 10–20 Myrs, the Nazca–South America rotation rate has decelerated by 0.04°–0.06 °/Myr^2.
© 2003 Elsevier Science Ltd. All rights reserved.

Keywords: Nazca–South American plate; Kinematic analysis; Euler vector

1. Introduction

The Cenozoic history of Nazca–South American (SoAm) plate convergence obtained by kinematic analysis of marine magnetic anomalies and plate circuit closure suggests that phases of intense tectonic activity in the Andes are associated with periods of rapid subduction (Pilger, 1983; Pardo-Casas and Molnar, 1987; Somoza, 1998). The most recent of these studies (Somoza, 1998) finds that subduction rates in the Central Andes near 22°S peaked at more than 150 mm/yr between 20 and 25 Ma and has steadily declined from 20 Ma to the present. Estimates of the present rate of subduction at 22°S lie in the range of 63–79 mm/yr.

Most estimates of the contemporary Nazca–SoAm convergence rate are based on the global kinematic model NUVEL-1A (DeMets et al., 1994) or geodetic measurements (Larson et al., 1997; Norabuena et al., 1998, 1999; Angermann et al., 1999). Angermann et al. (1999) were the first to recognize a major discrepancy between their

geodetic measurements and the predictions of NUVEL-1A. Their Nazca–SoAm Euler vector has an angular velocity of 0.59 °/Myr, compared with NUVEL-1A's value of 0.72 °/Myr, which thus implies a ~20% difference in the subduction rate in the Central Andes. Norabuena et al. (1999) suggest that, because NUVEL-1A averages plate motions over the past 3 Myrs, discrepancies between NUVEL-1A and geodetic studies of Nazca–SoAm convergence can be explained by the deceleration of plate convergence implicit in plate reconstructions. However, if we accept a Euler vector similar to that of Angermann et al. (1999), this explanation implies a rate reduction of approximately 20% in just 1.5 Myrs, considerably larger than the deceleration implied by the reconstructions of Somoza (1998).

Herein, we present two new Euler vectors (CAP09 and CAP10) for Nazca–SoAm derived from global positioning system (GPS) velocity fields measured by the Central Andes GPS Project (Kendrick et al., 1999; Bevis et al., 2001). The CAP09 and CAP10 vectors differ in the weights they assign to a problematic GPS station in Easter Island. However, both solutions are similar to the result obtained by Angermann et al. (1999), in that they imply subduction

---

* Corresponding author. Tel.: +1-808-956-7864; fax: +1-808-956-3188.
E-mail address: bevis@soest.hawaii.edu (M. Bevis).

rates approximately 20% lower than those predicted by NUVEL-1A. We use our preferred solution, CAP10, in combination with the plate reconstructions of Somoza (1998); Pardo-Casas and Molnar (1987), to estimate the rate of deceleration of Nazca–SoAm plate convergence during the past 10–20 Myrs.

2. The GPS velocity field

Our approach to GPS data analysis, reference frame realization, and velocity estimation has been described at length by Kendrick et al. (2001), so will not be repeated here. We update the analysis of Kendrick et al. (2001) by employing a longer time series. We present our latest velocity solutions in a reference frame that fixes the stable core of the SoAm plate. The RMS residual velocity of the ten SoAm stations used to realize this frame is just 0.7 mm/yr (Table 1). Nine of these stations are located in the continental crust, and one (ASC1 on Ascension Island) is located in oceanic crust near the eastern limit of the SoAm plate.

We obtained velocities for five stations in the Nazca plate: two continuous GPS (or CGPS) stations and three survey GPS (or SGPS) stations. The two CGPS stations— GALA (Santa Cruz Island) and EISL (Easter Island)—are part of the global network of the International GPS Service. Two of the three SGPS stations—FLIX (San Felix Island) and RBSN (Robinson Crusoe Island)—are part of the CAP network, and BALT (Baltra Island) is part of the Sistema de Referencia Geocentrico para America del Sur (SIRGAS) network. Our GPS stations on San Felix and Robinson Crusoe Islands are physically distinct from those measured

and used by Angermann et al. (1999). The velocities of these stations are listed in Table 1 and plotted in Fig. 1. The velocity vectors obtained at GALA and BALT, located approximately 32 km apart in the Galapagos Islands, are similar.

3. The present-day Nazca–SoAm Euler vector

The GPS stations on the Nazca plate, except RBSN, are located on or within ∼100 km of active volcanoes. Although there were no major eruptions near any of these stations during the course of the GPS measurements, we note that our geodetic velocity measurements may be contaminated by site instabilities, such as volcanic straining or slope instability. We assume that at each station the horizontal and vertical components of velocity due to site instability are zero mean stochastic variables with standard deviations of σ_h and σ_v, respectively. These supplementary uncertainties may vary from one station to another, and we assign their values a priori on a best-guess basis (see Tables 2 and 3) and use this information to augment or inflate the geodetic covariance matrices prior to using them to weight the various velocity estimates during the inversion for the Euler vector (see Appendix A for more details).

In our first treatment, the level of noise associated with site instability is assumed to be minor at all stations (Table 2). We inverted the velocity estimates to find the Euler vector designated CAP09 (Table 2, Fig. 2). The velocity residuals in the Nazca plate have an RMS magnitude of 2.6 mm/yr, with the largest residual, 3.5 mm/yr, at RBSN. A careful analysis of these residuals indicates that station EISL appears to be moving relative to

Table 1

The GPS velocity solutions used in this study. The table columns list the station name and position, the total time span of observation (years), the north component of velocity and its standard error, the east component of velocity and its standard error, the horizontal velocity magnitude (all in mm/yr), the correlation between the estimates of the north and east velocity components (which specifies the orientation of the error ellipse), and the station type (C = continuous, S = survey)

| Stnm	Lat	Lon	Tspan	v_n	σ_n	v_e	σ_e	v_h	C_{ne}	Type
Stations in stable core of South American Plate										
KOUR	5.25	−52.81	9.59	−0.4	0.1	0.2	0.2	0.4	0.019	C
FORT	−3.88	−38.43	8.66	−0.1	0.1	−0.3	0.2	0.4	0.045	C
ASC1	−7.95	−14.41	6.40	−0.8	0.2	−0.5	0.3	0.9	0.058	C
BRAZ	−15.95	−47.88	7.52	−0.1	0.1	0.6	0.2	0.6	0.046	C
UEPP	−22.12	−51.41	7.30	0.6	0.1	−0.4	0.2	0.7	−0.028	C
PARA	−25.45	−49.23	7.30	−0.1	0.1	−0.3	0.2	0.3	0.074	C
LPGS	−34.91	−57.93	8.65	−0.2	0.1	0.0	0.1	0.2	−0.119	C
TNDL	−37.32	−59.09	8.18	0.2	0.3	0.9	0.4	0.9	0.098	S
LHCL	−38.00	−65.60	5.81	−0.5	0.2	−0.1	0.1	0.5	−0.220	C
LKTH	−51.70	−57.85	3.93	1.1	0.2	0.3	0.1	1.1	−0.075	C
Stations in Nazca Plate										
BALT	−0.46	−90.26	6.32	3.2	0.3	53.8	0.5	53.9	0.001	S
GALA	−0.74	−90.30	6.61	2.3	0.1	55.9	0.2	56.0	0.000	C
FLIX	−26.30	−80.09	7.35	7.7	0.2	62.8	0.2	63.3	−0.128	S
EISL	−27.15	−109.38	8.64	−12.0	0.2	67.9	0.2	69.0	0.133	C
RBSN	−33.63	−78.84	6.68	7.8	0.6	62.5	0.4	63.0	−0.296	S
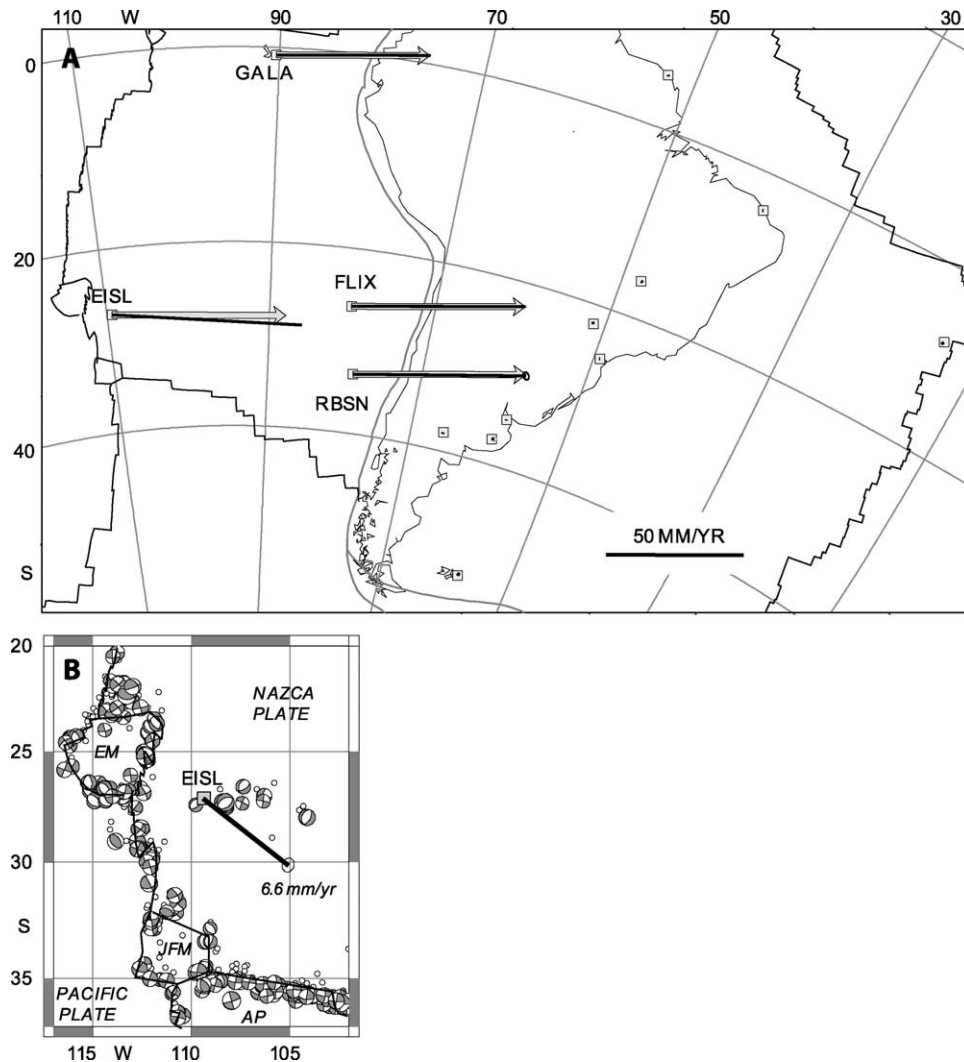
Fig. 1. (A) Crustal velocities relative to the stable South American plate (see Table 1). The GPS measurements are shown in black; in most cases, the 95% error ellipse (see RBSN) is too small to see at this scale. The velocities predicted by the CAP10 Euler vector (Table 1) are shown using grey arrows. We do not show the results from BALT on the Nazca plate because they overlap with those from the nearby station GALA. The results from GALA and BALT are very similar. (B) Interplate and intraplate seismicity near Easter Island. The arrow depicts the residual velocity (GPS-CAP10 prediction) at EISL and its 95% confidence ellipse. The focal mechanisms are from the Harvard CMT catalogue. EM = Easter microplate, JFM = Juan Fernandez microplate, and AP = Antarctic plate.

the other four stations on the Nazca plate. The anomalous motion of EISL is also apparent in Fig. 1A, in which the oblique Mercator map projection (centered near the Euler pole) is devised so that the Euler velocity field is very nearly horizontal (i.e. parallel to the top side of the map frame) everywhere on the map. This anomalous motion is much larger than would normally be associated with site instabilities, and it presents the possibility that Easter Island is located in a deforming plate boundary zone rather than in the stable core of the Nazca plate. Easter Island is situated on one of a suite of linear structures pervading the oceanic crust, some of which are seismically active (Fig. 1B), and much of the seafloor surrounding Easter Island is covered with recent volcanic material (Liu, 1996; D. Naar and P. Wessel, pers. comm.).

In response to these findings, we performed a second inversion for the Euler pole in which we eliminated

the influence of the EISL velocity by excluding it from the inversion. This leads to our preferred Euler vector, designated CAP10, as described in Table 3 and Fig. 2. We compared the velocities predicted by CAP10 with the observed velocities in Fig. 1 and Table 3. The velocity residual at EISL is increased to 6.6 mm/yr, bearing N128°E (Fig. 1B), but the residuals at the other four stations are less than 2 mm/yr, with an RMS value of just 1.0 mm/yr. Note that the residual velocity vector for EISL is very much larger than its error ellipse (Fig. 1B).

4. A comparison of Euler poles

We compare CAP09, CAP10, and four prior geodetic estimates for the present-day Nazca–SoAm Euler pole in Fig. 2. This figure also shows the NUVEL-1A pole and three

Table 2
Information related to solution CAP09 for the Nazca–SoAm Euler vector. The upper section lists by station the supplementary uncertainties (σ_h and σ_v) used to augment the covariance matrices associated with the GPS solutions, the velocities predicted by the Euler vector, and the associated velocity residuals (observed − computed). Velocity magnitudes (mag) are stated in mm/yr, and velocity azimuths (azm) are stated in degrees east of north. The Euler vector and its covariance matrix are provided in geocentric Cartesian coordinates with the units radians/year and (radians/year)^2. The pole and rate of rotation are stated in more familiar form

Station Code	σ_h	σ_v	Model velocity		Velocity residual	
			mag	azm	mag	azm
EISL	0.2	0.3	66.2	99.4	2.9	113.4
GALA	0.2	0.3	55.5	88.5	0.9	25.8
BALT	0.3	0.5	55.4	88.5	2.3	−41.8
FLIX	0.2	0.3	66.0	83.0	2.7	−97.7
RBSN	0.2	0.3	66.5	82.4	3.5	−107.2

Variance of unit weight = 6.09

	Euler vector	Covariance matrix		
X	-2.574×10^{-10}	1.396×10^{-20}	6.413×10^{-21}	2.403×10^{-21}
Y	-5.864×10^{-9}	6.413×10^{-21}	1.553×10^{-19}	4.804×10^{-20}
Z	8.631×10^{-9}	2.403×10^{-21}	4.804×10^{-20}	3.296×10^{-20}

Euler pole: geocentric Lat = 55.78, Long = −92.51; angular velocity = 0.598 ± 0.009 degrees/Myr.

finite rotation poles associated with the plate reconstructions of Somoza (1998) and Pardo-Casas and Molnar (1987).

The geodetically derived poles lie close to a great circle arc passing through or near their center of mass and the center of mass of the various GPS stations in the Nazca plate. This nearly north–south scatter is also reflected in the geometry of the various error ellipses. This scatter can be explained in part by a well-known instability that affects numerical estimates of Euler vectors: the pole may deviate toward (away from) the velocity sample sites and do relatively little damage to the fit of the observed and computed velocities if the rate of rotation is increased (decreased) commensurately. This trade-off is difficult to suppress unless the velocity field is sampled over a very wide range of Euler latitudes, which is not possible for small plates.

The NUVEL-1A pole, the CAP09 and CAP10 poles, and the pole of Angermann et al. (1999) are not significantly different at the 95% level of confidence. The CAP09 and CAP10 poles are the only geodetic estimates to lie very close to or north of the NUVEL-1A pole and close to the rotation poles of Somoza (1998) for anomaly 3 (4.9 Ma) and anomaly 5 (10.8 Ma). When these rotation poles are compared with the anomaly 5 pole of Pardo-Casas and Molnar (1987) and the NUVEL-1A pole, which represents a 3 Myr average, we find that we cannot identify with any reasonable confidence the direction in which the Euler pole has drifted during the past 10.8 Myrs, except perhaps that the drift has had an easterly component. No error ellipses were provided for the three finite rotation poles, but if they are of similar size to the NUVEL-1A error ellipse (or larger), we would conclude that these poles, NUVEL-1A's

Table 3
Our preferred solution CAP10 for the Nazca–SoAm Euler vector. This table follows the format of Table 2. Station EISL is no longer used to invert for the Euler vector

Station Code	σ_h	σ_v	Model velocity		Velocity residual	
			mag	azm	mag	azm
EISL	–	–	63.2	97.2	6.6	128.2
GALA	0.2	0.3	55.8	87.8	0.2	60.8
BALT	0.3	0.5	55.7	87.7	0.1	29.5
FLIX	0.2	0.3	63.2	83.1	0.1	29.5
RBSN	0.2	0.3	63.0	82.5	0.4	167.4

Variance of unit weight = 2.36

	Euler vector	Covariance matrix		
X	-3.680×10^{-10}	$+3.037 \times 10^{-21}$	-3.121×10^{-21}	-7.700×10^{-22}
Y	-4.797×10^{-9}	-3.121×10^{-21}	4.787×10^{-20}	1.119×10^{-20}
Z	8.681×10^{-9}	-7.700×10^{-22}	1.119×10^{-20}	6.452×10^{-21}

Euler pole: geocentric Lat = 61.01, Long = −94.39; angular velocity = 0.569 ± 0.005 degrees/Myr.
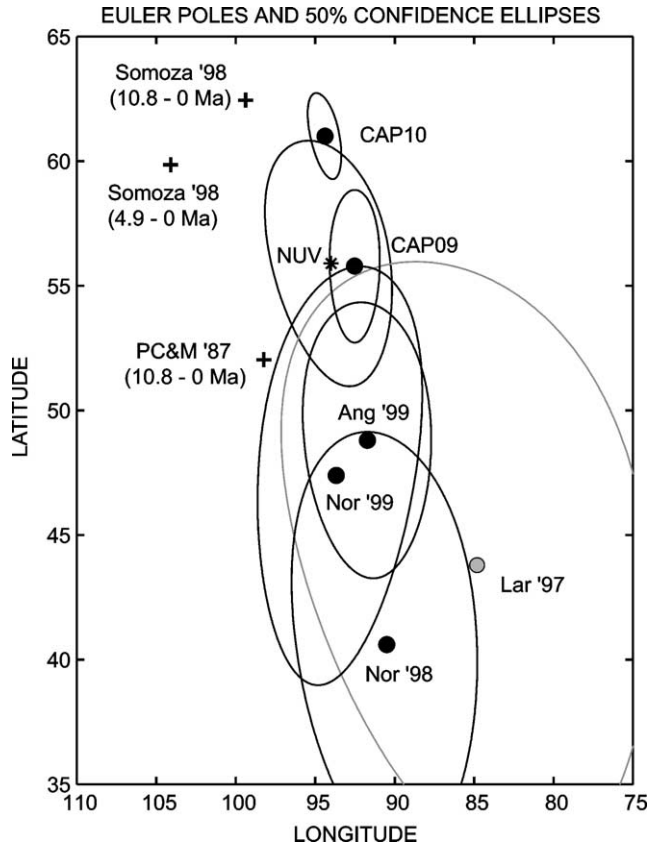
Fig. 2. Euler poles associated with NUVEL-1A (NUV); the finite rotations obtained by Somoza (1998) (Som98) and Pardo-Casas and Molnar (1987) (PC&M87) for 4.9–0 Ma (Somoza only) and 10.8–0 Ma; and the poles derived from GPS measurements by Larson et al. (1997) (Lar97), Norabuena et al. (1998) (Nor98), Angermann et al. (1999) (Ang99), Norabuena et al. (1999) (Nor99), and this article (CAP09, CAP10). All error ellipses are 50% confidence intervals. No error ellipses were reported by Som98 or PC&M87.

poles, and the CAP09 and CAP10 poles are statistically indistinguishable.

Our solutions CAP09 and CAP10 have rotation rates of 0.598 ± 0.009 and 0.569 ± 0.005 °/Myr, respectively. Both rates are close to the value of 0.59 ± 0.014 °/Myr reported by Angermann et al. (1999). Given this close agreement, we adopt the CAP10 rate for the present and compare it with average rates obtained from various stage poles to infer how the angular velocity of the Nazca–SoAm Euler vector has changed during the past ~20 Ma (Fig. 3). Estimating a deceleration in this way involves a familiar problem: If we estimate a rate over a shorter period of time (say, 10.8 Myrs), we are less likely to run into difficulties when we assume a constant rate of deceleration. However, by estimating a rate over a longer period of time (say, 20 Myrs) and incorporating additional measurements, we might better mitigate the impact of individual measurement errors. Because of the absence of error bars on many of the points in Fig. 3, we believe it would be premature to try to infer how the deceleration rate may have changed during the past 20 Myrs. We prefer to conclude simply that during the past 10–20 Myrs, the rate of rotation of the Nazca–SoAm Euler vector has declined or decelerated by
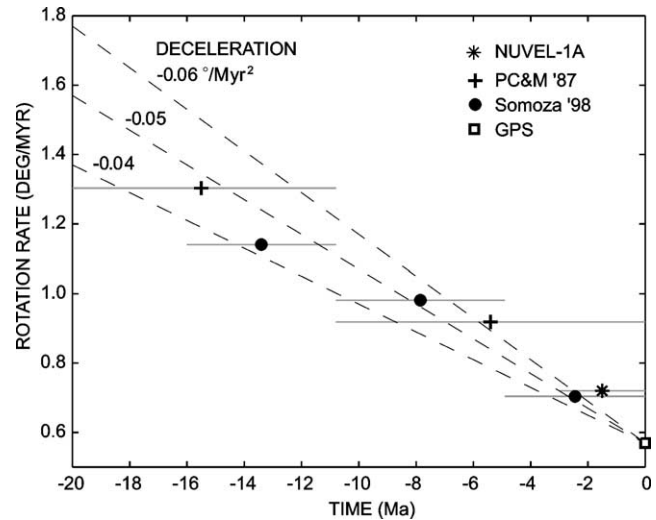

Fig. 3. The Nazca–SoAm rotation rate versus time. The average rotation rates implied by the various stage poles of Somoza (1998) and Pardo-Casas and Molnar (1987) are plotted at the midpoint of the averaging interval. The horizontal lines indicate the associated time intervals. Also shown is the NUVEL-1A rate and the GPS rate from CAP10. If we assume that Nazca–SoAm convergence has had a constant rate of deceleration from some epoch T to the present day, then the points plotted for times $\leq T$ should fall on one straight line. If we assume that our estimate of the present day rate is correct, then the family of dashed lines represents rotation rate versus time for three specific values of deceleration rate, as labeled. The error bars for NUVEL-1A and CAP10 are too small to be easily visible at the scale of the plot. No error bars are available for the remaining estimates of rotation rate.

between 0.04 and 0.06 °/Myr². We also conclude that the rotation rate difference between NUVEL-1A (i.e. 0.72 ± 0.02 °/Myr) and the three nearly identical geodetic estimates (CAP09, CAP10, and Angermann et al., 1999) is not easily explained by uniform deceleration of Nazca–SoAm plate convergence (Fig. 3).

5. Discussion

Each new estimate of the current Nazca–SoAm Euler pole is usually more tightly constrained than prior estimates by virtue of a steadily expanding data set. At this point, the major uncertainty is whether the GPS station at EISL is moving relative to the stable core of the Nazca plate. We believe it probably is, and for this reason, we prefer CAP10 to CAP09. We have no observational basis for deciding whether this anomalous motion is due to ground or monument instability, volcanic deformation, or regional intraplate deformation, though we suspect that regional deformation is the major problem.

The various geodetic estimates for the Nazca–SoAm Euler vector imply quite different subduction rates over the plate boundary as a whole (Table 4 and Fig. 4). Resolving these discrepancies has important implications for seismic risk along the Andes, as well as for groups modeling interseismic strain accumulation (e.g. Bevis et al., 2001; Trenkamp et al., 2002).

Table 4
Velocity of the Nazca plate relative to the South America plate predicted by
NUVEL-1A (DeMets et al., 1994) and recent geodetic estimates of the
Euler vector at a set of points lying close to the plate boundary. The two
subtables list the magnitude and bearing of the horizontal velocity predicted
at each point. Abbreviations for the Euler vectors are as follows:
Nuv = NUVEL-1A, Lar97 = Larson et al. (1997), Nor98 = Norabuena
et al. (1998), Ang99 = Angermann et al. (1999), and Nor99 = Norabuena
et al. (1999). CAP09 and CAP10 are derived in this article

Lat	Lon	Nuv	Lar97	Nor98	Ang99	Nor99	CAP09	CAP10
Horizontal velocity magnitude (mm/yr)								
+ 5.0	− 78.0	63.6	52.2	48.0	46.7	48.7	52.5	53.3
0.0	− 82.0	67.0	57.1	52.2	50.0	52.0	55.5	55.8
− 10.0	− 80.2	73.7	66.6	61.8	56.6	59.2	61.1	60.1
− 20.0	− 71.3	78.4	74.5	70.4	62.1	65.3	65.0	62.8
− 30.0	− 72.4	80.0	79.3	75.3	64.7	68.2	66.4	63.2
− 40.0	− 75.1	79.4	81.8	78.1	65.6	69.3	66.0	61.8
− 46.0	− 75.8	78.0	82.2	78.8	65.3	69.1	64.9	60.1
Horizontal velocity azimuth (N°E)								
+ 5.0	− 78.0	78.8	82.2	74.3	77.3	74.9	79.7	80.7
0.0	− 82.0	82.0	87.1	80.2	81.6	79.5	82.9	83.2
− 10.0	− 80.2	81.6	85.9	80.0	81.2	79.4	82.5	82.8
− 20.0	− 71.3	77.2	79.3	73.7	76.0	74.1	78.0	79.0
− 30.0	− 72.4	78.1	80.7	75.7	77.2	75.5	78.8	79.5
− 40.0	− 75.1	79.5	83.0	78.2	79.2	77.5	80.2	80.6
− 46.0	− 75.8	79.7	83.5	78.9	79.6	78.0	80.5	80.7

We estimate that the rate of rotation associated with the
Nazca–SoAm Euler vector has been decreasing by
approximately 0.04–0.06 °/Myr^2 for the past 10–20 Myr.
However, it is not possible to estimate the directional part of
the acceleration (deceleration) vector. This difficulty reflects
the uncertainties associated with plate reconstructions, as
much as it does those associated with geodetically inferred
Euler poles.

Acknowledgements

Appendix A

Let v_n represent the velocity of the Nazca plate at a given
station, v_i represent the much smaller velocity of the GPS
antenna or monument relative to the Nazca plate due to local
instabilities (e.g. volcanic straining, slope instabilities), and
v_g represent the total velocity of the antenna or monument.
(Both v_n and v_g are stated relative to the SoAm plate.) We
measure v_g but prefer to use v_n in our inversion for the Euler
pole. Now, $v_n = v_g − v_i$, but because we do not know the
value of v_i, we must equate it with the zero vector and set
$v_n = v_g$. Nevertheless, we can take some account of
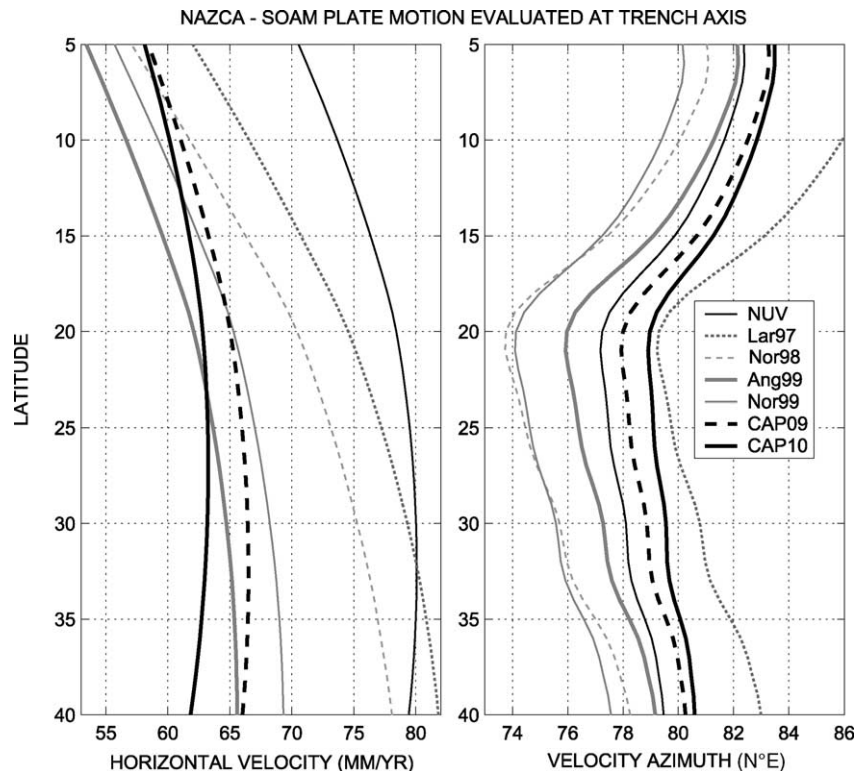the additional uncertainties introduced by potential site

Fig. 4. Velocity magnitude and direction along the Nazca–South America plate boundary between 5°S and 40°S, as predicted by NUVEL-1A and Euler vectors
inferred from geodetic measurements. The abbreviations are those used in Fig. 2 and Table 4.

instabilities. Suppose that σ_h and σ_v are the standard errors associated with the horizontal and vertical components of local velocity vector $\mathbf{v}_i$. By assigning nonzero values to σ_h and σ_v, we allow for the possibility that we may be in error when we assume that $\mathbf{v}_i$ has only zero elements. Let $\mathbf{C}_n$, $\mathbf{C}_g$, and $\mathbf{C}_i$ be the covariance matrices for $\mathbf{v}_n$, $\mathbf{v}_g$, and $\mathbf{v}_i$, respectively. Then, $\mathbf{C}_n = \mathbf{C}_g + \mathbf{C}_i$. To take potential site instabilities into account, we use the augmented covariance matrix $\mathbf{C}_n$ rather than the geodetic covariance matrix $\mathbf{C}_g$ during our inversion for the Euler vector. We assume that in local topocentric (east, north, up) coordinates, $\mathbf{C}_i$ is a diagonal matrix with diagonal elements σ_h^2, σ_h^2, and σ_v^2. (If we set $\sigma_h = \sigma_v = 0$, $\mathbf{C}_n$ reduces to $\mathbf{C}_g$.) The supplementary velocity uncertainties σ_h and σ_v used in our inversions are listed by station in Tables 2 and 3.

References

Angermann, D., Klotz, J., Reigber, C., 1999. Space-geodetic estimation of the Nazca–South America Euler vector. Earth Planet. Sci. Lett. 171, 329–334.

Bevis, M., Kendrick, E., Smalley, R., Brooks, B., Allmendinger, R., Isacks, B., 2001. On the strength of interplate coupling and the rate of backarc convergence in the Central Andes: an analysis of the interseismic velocity field. Geochem. Geophys. Geosyst. 2 Paper 2001GC000198.

DeMets, C., Gordon, R.G., Argus, F., Stein, S., 1994. Effect of recent revisions of the geomagnetic timescale on estimates of current plate motions. Geophys. Res. Lett. 21, 2191–2194.

Kendrick, E., Bevis, M., Smalley, R., Cifuentes, O., Galban, F., 1999. Current rates of convergence across the Central Andes: estimates from continuous GPS observations. Geophys. Res. Lett. 26, 541–544.

Kendrick, E., Bevis, M., Smalley, R., Brooks, B., 2001. An integrated crustal velocity field for the Central Andes. Geochem. Geophys. Geosyst. 2 Paper 2001GC000191.

Larson, K., Freymueller, J., Philipsen, S., 1997. Global plate velocities from the global positioning system. J. Geophys. Res. 102, 9961–9981.

Liu, Z., 1996. The origin and evolution of the Easter seamount chain. Unpublished PhD Thesis, University of South Florida, 266 p

Norabuena, E., Leffler-Griffin, L., Mao, A., Dixon, T., Stein, S., Sacks, I., Ocala, L., Ellis, M., 1998. Space geodetic observation of Nazca–South America convergence across the Central Andes. Science 279, 358–362.

Norabuena, E., Dixon, T., Stein, S., Harrison, C.G.A., 1999. Decelerating Nazca–South America and Nazca–Pacific motions. Geophys. Res. Lett. 26, 3405–3408.

Pardo-Casas, F., Molnar, P., 1987. Relative motion of the Nazca (Farallon) and South American Plate since Late Cretaceous time. Tectonics 6, 233–248.

Pilger, R., 1983. Kinematics of the South America subduction zone from global plate reconstructions. In: Cabre, R., (Ed.), Geodynamics of the Eastern Pacific Region, Caribbean and Scotia Arcs, Geodynamics Series 9, American Geophysical Union, Washington DC, pp. 113–1256.

Somoza, R., 1998. Updated Nazca (Farallon)–South America relative motions during the last 40 My: implications for mountain building in the central Andean region. J. S AM. Earth Sci. 11, 211–215.

Trenkamp, R., Kellogg, J.N., Freymueller, J., Mora, H., 2002. Wide plate margin deformation, southern Central America and northwestern South America, CASA GPS observations. J. S AM. Earth Sci. 15, 157–171.